

Exploring the Western Shoreline of the Nuclear Chart: What Precision Mass Spectrometry with TITAN-TRIUMF Can Teach Us About Nuclear Existence

[Annabelle Czihalý](#)^{*}, [Soenke Beck](#), Julian Bergmann, Callum L. Brown, [Thomas Brunner](#), [Timo Dickel](#), [Jens Dilling](#), Eleanor Dunling, Jake Flowerdew, Zach Hockenbery, Andrew Jacobs, Brian Kootte, Stephan Malbrunot-Ettenauer, [Fernando Maldonado Millán](#), Ali Mollaebrami, Erich Leistenschneider, Eleni Marina Lykiardopoulou, Ish Mukul, Stefan F. Paul, [Wolfgang R. Plaß](#), [Moritz Pascal Reiter](#), Christoph Scheidenberger, James L. Tracy, Jr., A. A. Kwiatkowski

Posted Date: 5 September 2024

doi: 10.20944/preprints202409.0472.v1

Keywords: Mass spectrometry; proton dripline; time-of-flight mass spectrometry; ion traps; radioactive ion beams; experimental nuclear physics




Preprints.org is a free multidiscipline platform providing preprint service that is dedicated to making early versions of research outputs permanently available and citable. Preprints posted at Preprints.org appear in Web of Science, Crossref, Google Scholar, Scilit, Europe PMC.

Copyright: This is an open access article distributed under the Creative Commons Attribution License which permits unrestricted use, distribution, and reproduction in any medium, provided the original work is properly cited.

Article

Exploring the Western Shoreline of the Nuclear Chart: What Precision Mass Spectrometry with TITAN-TRIUMF Can Teach Us about Nuclear Existence

Annabelle Czihaly ^{1,2,*} , Sönke Beck ^{3,4}, Julian Bergmann ³, Callum L. Brown ⁵, Thomas Brunner ^{1,6}, Timo Dickel ^{3,4}, Jens Dilling ^{1,7}, Eleanor Dunling ^{1,8}, Jake Flowerdew ^{1,9}, Danny Fusco ^{1,10}, Leigh Graham ¹, Zach Hockenbery ^{1,6}, Chris Izzo ¹, Andrew Jacobs ^{1,7}, Brian Kootte ^{1,11}, Yang Lan ^{1,7}, Stephan Malbrunot-Ettenauer ¹², Fernando Maldonado Millán ¹, Ali Mollaebrahimi ^{1,3,4}, Erich Leistenschneider ^{1,7}, Eleni Marina Lykiardopoulou ^{1,7}, Ish Mukul ¹, Stefan F. Paul ^{1,13}, Wolfgang R. Plaß ^{3,4}, Moritz P. Reiter ^{1,3,5}, Christoph Scheidenberger ^{3,4,14}, James L. Tracy, Jr. ¹, and A. A. Kwiatkowski ^{1,2}

¹ TRIUMF, 4004 Wesbrook Mall, Vancouver, BC, Canada

² University of Victoria, 3800 Finnerty Rd, Victoria, BC, Canada

³ Justus-Liebig-Universität Gießen, 35392 Gießen, Germany

⁴ GSI Helmholtz Centre for Heavy Ion Research Planckstraße 1, 64291 Darmstadt, Germany

⁵ The University of Edinburgh, Old College, South Bridge, Edinburgh EH8 9YL, United Kingdom

⁶ McGill University, 845 Rue Sherbrooke O, Montréal, QC, Canada

⁷ The University of British Columbia, 2329 West Mall, Vancouver, BC, Canada

⁸ University of York, Heslington, York YO10 5DD, United Kingdom

⁹ University of Calgary, 2500 University Dr NW, Calgary, AB, Canada, T2N 1N4

¹⁰ University of Waterloo, 200 University Ave W, Waterloo, ON, Canada, N2L 3G1

¹¹ University of Manitoba, 66 Chancellors Cir, Winnipeg, MB, Canada, R3T 2N2

¹² CERN, CH-1211 Geneva 23, Switzerland

¹³ Heidelberg University, Grabengasse 1, 69117 Heidelberg, Germany

¹⁴ Helmholtz Forschungsakademie Hessen für FAIR (HFHF), GSI Helmholtzzentrum für Schwerionenforschung, Campus Gießen, 35392 Gießen, Germany

* Correspondence: aczihaly@triumf.ca

Abstract: Isotopes at the limits of nuclear existence are of great interest for their critical role in nuclear astrophysical reactions and their exotic structure. Experimentally, exotic nuclides are challenging to address due to low production cross-sections, overwhelming amounts of contamination, and lifetimes typically less than a second. To this end, a Multiple-Reflection Time-of-Flight mass spectrometer at the TITAN-TRIUMF facility was built to determine atomic masses. This device is a preferred tool to work with exotic nuclides due to its ability to resolve the species of interest from contamination and short measurement cycle times enabling mass measurements of isotopes with millisecond half-lives. With a relative precision of order 10^{-7} , we demonstrate why the TITAN MR-TOF MS is the tool of choice for precision mass surveys for nuclear structure and astrophysics. The capabilities of the device are showcased in this work including new mass measurements of short-lived tin isotopes ($^{104-107}\text{Sn}$) approaching the proton dripline as well as ^{89}Zr , ^{90}Y , and ^{91}Y . The last three illustrate how the broadband surveys of MR-TOF MS reach beyond the species of immediate interest.

Keywords: mass spectrometry; proton dripline; time-of-flight mass spectrometry; ion traps; radioactive ion beams; experimental nuclear physics

1. Introduction

The ratio of protons to neutrons as well as their total number determines the nuclear properties of any nuclide. The limits of stability or the point of being nuclear unbound is called the proton and neutron driplines. To understand the evolution of nuclear structure, and therefore the subatomic forces at play, is an outstanding challenge of intrinsic interest that also impacts studies of, for example, nuclear astrophysics. To approach the driplines experimentally invokes a number of obstacles: low production

cross-sections, substantial contamination, and short half-lives. High-sensitivity, -purification, and -speed methodologies are required. These traits characterize Multiple-Reflection Time-Of-Flight Mass Spectrometers (MR-TOF MSs).

The MR-TOF MS [1,2] at TRIUMF's Ion Trap for Atomic and Nuclear science (TITAN) [3] facility was constructed to focus on mass surveys to benefit studies of nuclear structure and nuclear astrophysics, where the required relative precisions are 10^{-6} and 10^{-7} , respectively. In this quest, the TITAN MR-TOF MS has reached precisions down to 9×10^{-8} [4], removed contamination up to 10^8 [1] times greater than the species of interest, and achieved sensitivities of rates as low as 0.007 detected ions per second [5]. Consequently, experiments towards the driplines occur increasingly frequently at the TITAN facility.

To this end, we detail an experiment aimed at exploring the nuclear structure of neutron-deficient tin isotopes towards the proton dripline. Herein, we report mass determinations of $^{104-107}\text{Sn}$, showcasing how the MR-TOF MS can be used to reduce contamination and obtain meaningful precisions in less than ten hours runtime. In addition, we document simultaneous mass measurements of ^{89}Zr , ^{90}Y , and ^{91}Y . These three were measured due to the broadband (i.e. non-resonant) technique of the MR-TOF MS.

2. Experimental Overview

The TITAN MR-TOF MS is based on the established setup Giessen-GSI FRS MR-TOF [6–8]. Similar devices are employed at, for example, RIKEN in Japan [9], CERN in Switzerland [10], and GSI in Germany [6], with typical relative precisions of 10^{-7} , although better can be achieved [11]. Recent exploits of the TITAN MR-TOF MS include measuring exotic neon isotopes [12], neutron-rich scandium isotopes [13], neutron-deficient ytterbium [14], and neutron-deficient nuclei in the $Z = 70 - 82$ region [15].

Radioactive ion beams (RIBs) are produced via the Isotope Separation On-Line (ISOL) method, by impinging a 480 MeV proton beam onto a thick target, causing fragmentation and spallation reactions. The radionuclides diffuse out of the $\approx 2000^\circ\text{C}$ target and are ionized by one of three ion sources at ISAC-TRIUMF [16]. For the neutron-deficient tin experiment, a proton beam current of $55 \mu\text{A}$ was used, incident on a tantalum target, and the Sn isotopes were selectively ionized by TRIUMF's Resonant Laser Ion Source (TRILIS) [17]. The beam is then sent through a dipole magnet, with a resolving power of approximately 2500 [16], eliminating species differing their ratio of mass number to charge state.

The RIB is then transported to TITAN's helium-gas-filled Radio Frequency Quadrupole (RFQ) ion trap [18]. The beam is cooled via successive collisions with the inert buffer gas with the RF field providing transverse confinement. An electrostatic gradient transfers the ions into the bunching region, where beam is accumulated and then extracted as ion bunches which are subsequently sent to the MR-TOF MS.

The MR-TOF MS [1] is composed of two main sections, a preparation section and an analyzer section (see Figure 1).

The preparation system is made of a series of helium-buffer-gas-filled RFQs [19]. The bunched beam passes through the input RFQ ion guide, through the RFQ switch-yard, past the transfer RFQ, and into the preparation trap (a linear Paul trap), where it is re-cooled. Next, the beam emittance is shaped in the injection trap before injection into the analyzer section.

The analyzer section is made of a pair of electrostatic mirrors, each four cylindrical electrodes, separated by a drift tube. A dynamic Time Focus Shift (TFS) is done to align the bunch's time focus with the downstream detector to maximize the temporal resolution. Each subsequent turn (i.e. after the first TFS turn) is an isochronous turn (IT). For this experiment, the ions underwent between 385 and 398 ITs in order to best separate the tin ions from isobaric contaminants. After completing their flight, the ions are ejected from the analyzer by opening the mirror closest to the detector. An ETP

MagneTOF™, measures the time of flight (TOF) of the ions. The measured TOF is used to deduce the mass via:

$$\frac{m}{z} = \frac{c \cdot (t - t_0)^2}{(1 + N_{IT} \cdot b)} \quad (1)$$

with z being the charge state, c , b , and t_0 being calibration parameters, and N_{IT} are the number of isochronous turns. Tune-specific parameters c and t_0 were determined prior to the experiment with well-known, stable ions. For the described experiment, $^{133}\text{Cs}^+$ from the MR-TOF MS thermal ion source was utilized and merged with the RIB via the RF switch-yard. For the determination of b , a time-resolved calibration (TRC) [20] is done using a high-statistics reference peak which corrects drifts in the time-of-flight spectra caused by, for example, diurnal temperature cycles in the experimental hall. TRCs further improve the achievable resolving power and, therefore, the separation of the ion of interest (IOI) from the contamination inherent to RIB production.

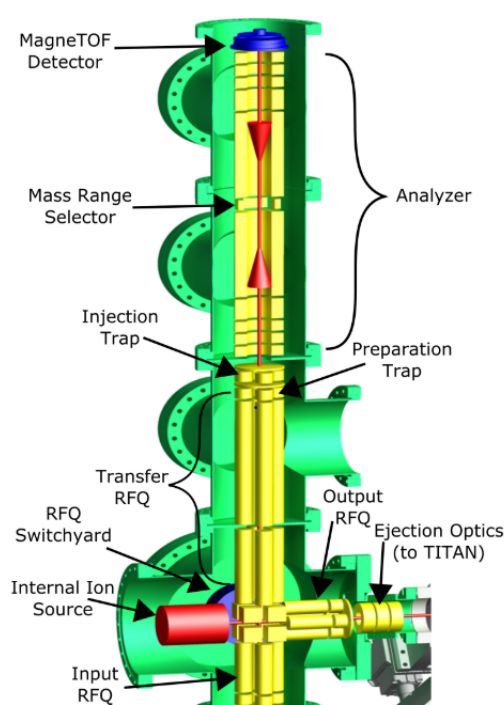


Figure 1. Schematic of the TITAN MR-TOF MS, highlighting primary components including the internal ion source, RFQ switch-yard, and analyzer. The unique combination allows the TITAN MR-TOF MS to merge calibrants with RIB and to act as its own beam purifier.

To reduce contamination, ions can be mass-selectively re-trapped [14]. Once ions are temporally separated in the analyzer, the IOI are re-trapped in the injection trap while the contaminants are deflected. The ions from the injection trap are re-cooled and re-injected into the analyzer, complete another TFS and more ITs, and are ejected for mass measurement. In the tin experiment, the dominant contaminants were atomic In^+ , Pd^+ , and Ag^+ as well as molecular Zr^{16}O^+ , Sr^{19}F^+ , and Y^{16}O^+ as seen in Figure 2, where the detected rate was as low as 0.02 particle per second (pps) for $^{104}\text{Sn}^+$.

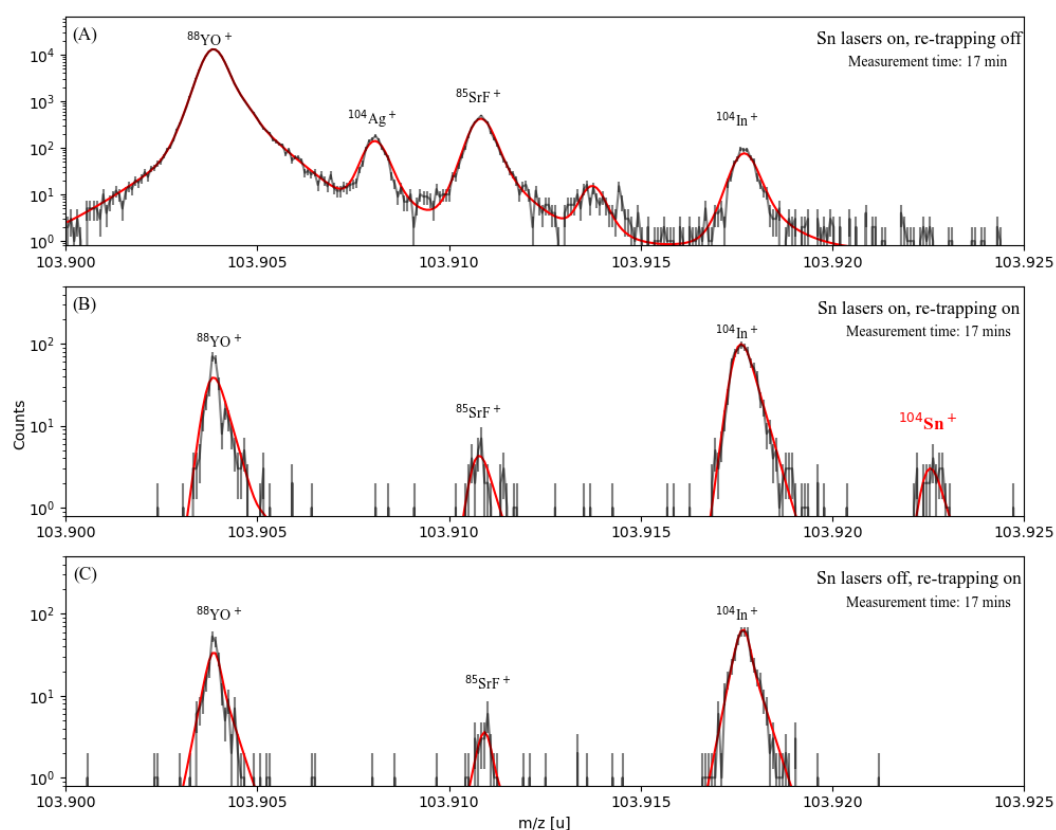


Figure 2. Spectra showing the effects of in-situ beam purification by re-trapping (off: panel A; on: panel B, panel C) and Sn-ionizing laser beams (blocked: panel C; unblocked: panel A, panel B) at $A = 104$. Without re-trapping, the tin isotopes cannot be observed, while the lasers provided an additional elemental confirmation of their identity.

In cases like this tin experiment, the elemental selectivity of TRILIS unambiguously reaffirms the identity of the IOI by comparing spectra with lasers on and off. In Figure 2 panel C, the peak of ^{104}Sn completely disappears in the absence of its resonant ionization by lasers.

3. Data Analysis

The data analysis follows the procedure described in [20] and is performed in two stages. First, TOF Control software [21] is used to obtain the time-resolved calibration. Spectra are broken down into calibration blocks and the peak of a well-known species in each block is fit with a Gaussian distribution and as a result, the time-dependent constant b is determined for each block.

Second, a fitting package, emgfit [22], employs exponentially modified Gaussian (hyper-EMG) distributions [20] for peak fitting. For each mass spectra, a well-resolved, high-statistics peak was selected to be the peak shape calibrant. For this analysis, isobaric $^8\text{In}^+$ was chosen. Since the $^8\text{In}^+$ peaks were broadened due to non-resolved isomers ($^m\text{In}^+$) the spacing between $^8\text{In}^+$ and $^m\text{In}^+$ were fixed parameters in the fitting procedure [23]. The shape calibrant was individually fit using Pearson's chi-squared statistic, minimizing the χ^2_P cost function. The shape-calibrant peak was fit with hyper-EMG distributions. Then, all peaks in the spectra were fit with the Poisson maximum likelihood estimation method (MLE). Here, MLE was preferred over chi-squared due to chi-squared biasing the mean in instances of low counts whereas MLE remained unbiased by implicitly assuming a Poisson distribution.

The ionic mass values, m_{ion} , were determined by

$$m_{\text{ion}} = \frac{(m/z)_{\text{cal,lit}}}{(m/z)_{\text{cal,MLE}}} \cdot (m/z)_{\text{MLE}} \cdot z \quad (2)$$

where $(m/z)_{\text{cal,lit}}$ is the literature mass obtained from AME2020 of the calibrant, $(m/z)_{\text{cal,MLE}}$ is the fitted mass of the calibrant, $(m/z)_{\text{MLE}}$ is the fitted mass of the ion of interest, and z is the charge state of the ion. The mass calibrants for this analysis are specified as “Mass Calibrant” in Table 1. The electron binding energies are negligible (as they are on the order of tens of electron volts) relative to the statistical uncertainty. Lastly, the atomic mass excess ME was determined by

$$ME = m_{\text{ion}} + z \cdot m_e - A \cdot u \tag{3}$$

where m_e is the mass of an electron, A is the mass number (total number of protons and neutrons), and u is the atomic mass unit.

The mass uncertainties were determined by quadratically summing the uncertainty from the fitting procedure to the systematic uncertainty. The systematic error, determined offline to be $\delta m/m = 3 \times 10^{-7}$, was dominated by the (voltage) ringing of the detector-side mirror’s electrodes which could have affected the extraction potential towards the detector. Any effect from ion-ion interactions inside the MR-TOF MS was negligible as measurements were performed with one ion per cycle.

Table 1. Summary of the mass excess ME values determined in this work and comparison to literature values obtained from AME2020 [24]. Number of detected events, calibrant species, and ionic mass ratios are presented.

Nuclide	Number of Events	Ionic Mass Ratio*	Mass Calibrant	ME _{TITAN} (keV)	ME _{AME} (keV)	Difference (keV)
⁸⁹ Zr	448	1.00002898(488)	⁸⁹ Y ¹⁶ O	-84883(35)	-84878(3)	5.2(35)
^{90g} Y	370	1.000023135(558)	⁹⁰ Zr ¹⁶ O	-86498(40)	-86497(0.4)	0.6(40)
^{90m} Y	266	1.000030123(563)	⁹⁰ Zr ¹⁶ O	-85805(41)	-85815(0.4)	10(41)
^{91g} Y	36797	1.000015435(464)	⁹⁰ Zr ⁹¹ O	-86351(33)	-86351(2)	0.7(33)
^{91m} Y	9328	1.000021048(476)	⁹⁰ Zr ¹⁶ O	-85797(35)	-85796(2)	1(35)
¹⁰⁴ Sn	101	1.00018007(624)	⁸⁸ Y ¹⁶ O	-71601(50)	-71627(6)	26(50)
¹⁰⁵ Sn	626	1.000195519(483)	⁸⁹ Y ¹⁶ O	-73349(34)	-73338(4)	-11(34)
¹⁰⁶ Sn	776	1.000164119(546)	⁹⁰ Zr ¹⁶ O	-77327(37)	-77354(5)	26(37)
¹⁰⁷ Sn	350	1.000141815(476)	⁹¹ Zr ¹⁶ O	-78511(34)	-78512(5)	1(34)

*Ionic Mass Ratios were determined from $m_{\text{IOI}} / m_{\text{cal}}$. For ^AY and ^AZr, since they were measured in molecular form, this ratio was determined using the ionic mass of the molecule of interest divided by the ionic mass of the molecular calibrant (e.g. $m_{\text{89Zr}^{16}\text{O}^+} / m_{\text{89Y}^{16}\text{O}^+}$). Errors in ionic mass ratios are given to their decimal place e.g., 1.00002898(488) = 1.00002898 ± 0.00000488.

4. Results

The mass values for exotic ^{104–107}Sn are detailed in Table 1 and compared to the AME2020 [24] values.

The TITAN and evaluated [24] tin values are found to be in excellent agreement (<1σ) with the latter based on Penning-trap mass determinations [25,26]. A comparison of the two ion-trap methodologies leads to two conclusions. First, the MR-TOF MS achieves superior speed, sensitivity, and dynamic range as has been demonstrated at TITAN (e.g. this work) and elsewhere (e.g. [27,28]). Second, while Penning trap mass spectrometry can achieve vastly superior precision, MR-TOF MS achieves sufficient precision for nuclear-structure and -astrophysics investigations.

To demonstrate the precision required for nuclear-structure studies, we calculated the two-neutron separation energy S_{2n} of the relevant tin isotopes:

$$S_{2n} = M(Z, N - 2) - M(Z, N) + 2M_n \tag{4}$$

where M_n is the mass of a neutron. In general, S_{2n} ranges from zero (neutron dripline) to tens of MeV (proton dripline), see e.g. Figure 3 of the tin region of interest. Typical behavior of the S_{2n} topology can be most easily understood through the nuclear shell model [29], wherein dramatically more stability is found at certain occupation (or "magic") numbers like neutron numbers $N = 2, 8, 20, 28, 50, 82, 126$. Partially filled shells manifest as a near linear trend in S_{2n} , a sharp discontinuity at closed shells, and more complicated behavior for highly deformed nuclei. The uncertainties achieved in this TITAN MR-TOF MS experiment (and all others) are adequate to probe nuclear shells and the evolution of nuclear structure towards the driplines.

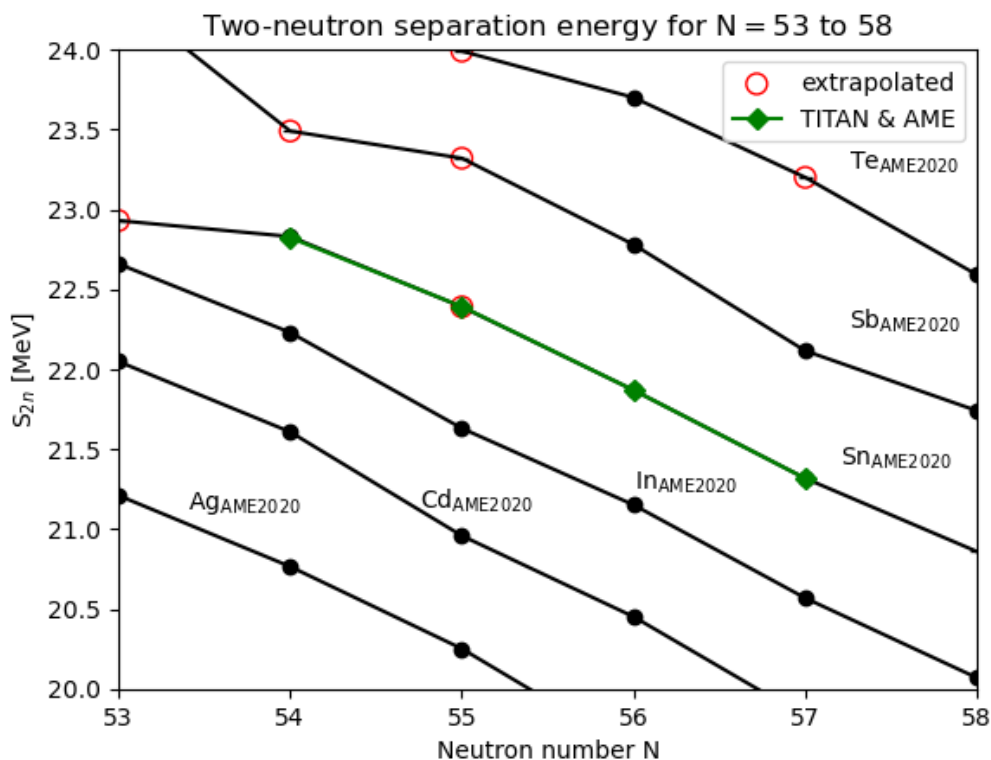


Figure 3. Surveys of the two-neutron separation energy S_{2n} are a common method to examine the evolution of nuclear structure; as the vertical axis scale indicates, the desired precision is less than about 100 keV to, well within reach of the MR-TOF MS. The TITAN values have been combined with AME values in this plot, seen in green, with a variance weighted mean. Red circles indicate values extrapolated from the mass surface by the authors of AME2020.

Success in measuring highly exotic species towards or at the driplines depends on the sensitivity of the MR-TOF MS. The lowest rate of detected ions in the tin experiment is 0.02 pps and in other TITAN experiments down to 0.0007 pps [5]. This sensitivity is in large part due to the in-situ beam purification or re-trapping method (described above), which can in milliseconds remove decades of contamination. While TITAN practice is to aim for at least 10 ions per IOI peak, as little as one ion suffices [27] and underscores the importance single-ion sensitivity and methodologies in addition to beam purification. As such, the MR-TOF MS can capture high RIB rates, purify the IOI (Figure 2), and then perform the mass measurement without ion-ion interactions.

Contamination poses two obstacles: obscuring the IOI and introducing a systematic shift in the measured mass due to ion-ion interactions. In the tin experiment, re-trapping reduced the maximum ratio of IOI to contamination from about $1:10^2$ to at most $1:30$ (e.g. see Figure 2a and b). For more typical re-trapping scenarios, the dynamic range exceeds the space-charge limit of any precision Penning trap mass spectrometer [30] and can only be matched by TOF spectrometers [31,32]. The former often relies on identifying contaminants *on-line* and then cleaning them individually (see [30]

and references therein). As such, substantial time is lost to preparing (rather than measuring) the IOI. The latter can sustain high space charge and is broadband and can be divided into so-called $B\rho$ -TOF and storage-ring-based measurements. $B\rho$ -TOF can reach single-ion sensitivity and a precision similar to the MR-TOF; however, the complexity of the calibration, often times requiring many well-known masses, can pose a significant challenge. For TOF experiments in a storage ring to achieve single-ion sensitivity and a precision comparable to the MR-TOF, the required beam cooling raises the lower limit in half-life to of order one second, about 200 times higher than demonstrated at the TITAN MR-TOF MS of 6 ms [4].

Capable of half-lives of a few ms, the MR-TOF MS is well suited to measurements approaching the driplines although in the neutron-deficient Sn isotopes, half-lives range from a few to tens of seconds due to their “magic” nature (of the closed proton shell). The half-life (here at least 21 seconds for ^{104}Sn [23]) along with the expected yield and contamination rate determine the MR-TOF MS duty cycle prepared for each experiment. The short duty cycles and the sensitivity allow for fast measurements; the duration of this experiment was about 10 hours, and the total data taking a mere four hours.

5. Discussion on Direct and Indirect Mass Measurements

In the tin isotopes, the next neutron-deficient isotope, ^{103}Sn , has only been measured indirectly through its β -endpoint energy [33,34]. Both measurements have been discarded by the AME2020 authors (see pp. 21-22 of [35] for full discussion) because the trends in the mass surface indicate ^{103}Sn should be 120 keV more bound. In β -endpoint energy measurements, systematic errors like the pandemonium effect [36] can be significant. Yet, β -endpoint measurements were often the best historical means to deduce masses of highly unstable nuclides. In another example, ^{90}Br is separated from stability by five β^- decays, with its β -endpoint energy being first measured in 1981 [37]. These Q_{β^-} values were measured (see [24] and references therein) towards stability up to ^{90}Y , which was determined through (n,γ) and (d,p) measurements from stable ^{89}Y (see [24] and references therein); that is, in 1981 the measured mass of ^{90}Br depended on the mass determination of four other short-lived species. When the mass of ^{90}Br and its daughter were directly measured [38,39], the determined Q_{β^-} -value deviated from the 1981 value by 1.2 MeV or 2.9σ ! The discrepancy in the β -endpoint energies measured for ^{90}Br and ^{103}Sn underscore the need for accuracy, typically best achieved by direct techniques. For this reason, we present herein the first direct mass measurements of ^{89}Zr and $^{90,91}\text{Y}$.

In comparing the neighborhood of ^{89}Zr and $^{90,91}\text{Y}$ with that of $^{104-107}\text{Sn}$ in Figure 4, their simultaneous measurement may appear unlikely. However, the Zr and Y formed oxide molecules and were delivered to TITAN as molecular ions; consequently, they were isobars of the tin IOI. Their simultaneous measurement was enabled by the broadband or non-resonant nature of MR-TOF MS. (The molecular bond is negligible relative to the statistical uncertainty.) In all three cases, good agreement was found between the TITAN and AME2020 values, and the TITAN ^{91}Y value will be a modest improvement in future mass evaluations. This experiment demonstrates how the contamination inherent to RIB production may allow additional measurements of nuclides which were formerly known only by indirect measurements (this work) or can anchor a chain of indirect measurements [15]. Surprisingly, many nuclides near stability have been measured only indirectly (see Figure 4) despite their value in verifying trends in the mass surface and therefore our understanding in nuclear structure.

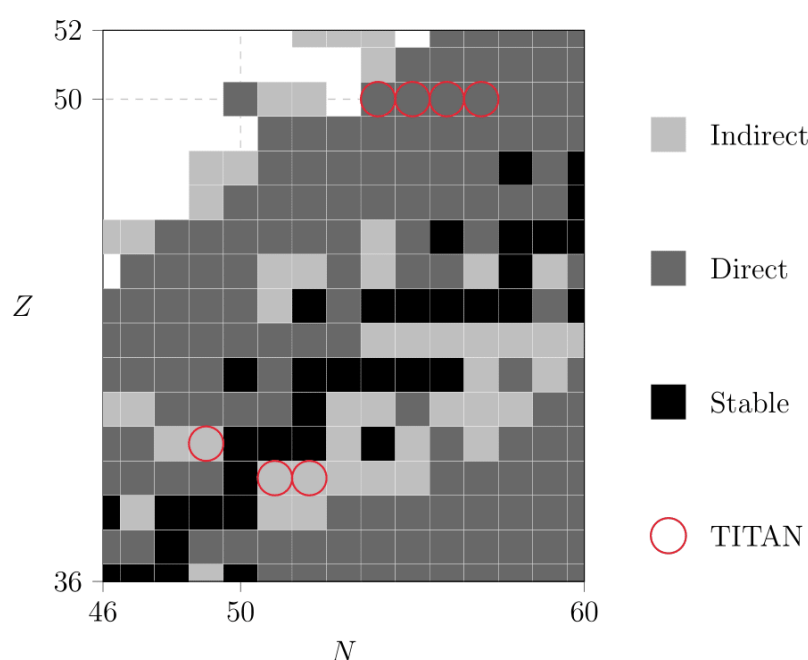


Figure 4. The section of the chart of nuclides relevant to this article displayed by measurement type listed in the AME2020 [24]; see text for more information. Tens of nuclides have had their masses measured only indirectly (light gray) despite being adjacent to so-called “valley of stability.” Three of these – ^{89}Zr , $^{90,91}\text{Y}$ – have been measured in this work (red circles), despite the focus on the neutron-deficient tin isotopes. These measurements were possible due to the broadband nature of the MR-TOF MS.

6. Summary and Outlook

High-precision mass measurements of neutron-deficient tin isotopes as well as first-time direct measurements of ^{89}Zr and $^{90,91}\text{Y}$ were performed at TITAN-TRIUMF using the MR-TOF MS technique. All results confirmed the AME2020 values within 1σ in only four hours of measurement time, a fraction of the time required for Penning trap mass spectrometry, which was previously used to explore this region.

The experiment showcases the capabilities of the MR-TOF MS to meet the challenges of surveying towards and along the nuclear driplines: duty cycles compatible with half-lives of only a couple milliseconds; at TITAN, half-lives as low as 6 ms have been measured. High resolving powers separate the species of interest from contaminants; at TITAN, resolving power up to 600,000 have been demonstrated [40] with ongoing efforts for higher. Finally re-trapping permits a dynamic range as large as $1 : 10^8$ to measure species with detected rates as low as 0.0007 pps. Finally, MR-TOF MS is a broadband, non-resonant technique that can allow the simultaneous mass cartography of nearby regions of interest. These factors and a typical precision of $\sim 10^{-7}$ make the MR-TOF MS an ideal instrument to survey the driplines. Such measurements are of the highest priority to understand the evolution of nuclear structure and explosive nucleosynthesis, where sensitivity, precision, and accuracy are critical.

Author Contributions: Conceptualization, Thomas Brunner and A. A. Kwiatkowski; Data curation, Julian Bergmann and Stefan Paul; Formal analysis, Annabelle Czihalý; Funding acquisition, Thomas Brunner, Jens Dilling, Stephan Malbrunot-Ettenauer, Moritz Reiter and A. A. Kwiatkowski; Investigation, Soenke Beck, Eleanor Dunling, Jake Flowerdew, Zach Hockenbery, Andrew Jacobs, Brian Kootte, Erich Leistenschneider, Eleni Marina Lykiardopoulou, Ish Mukul, Stefan Paul, Moritz Reiter and James Tracy, Jr.; Software, Julian Bergmann, Stefan Paul, Wolfgang Plaß and Christoph Scheidenberger; Supervision, A. A. Kwiatkowski; Validation, Fernando Maldonado Millán, Ali Mollaebrahimi and Moritz Reiter; Visualization, Callum Brown; Writing – original draft, Annabelle Czihalý; Writing – review & editing, Annabelle Czihalý, Timo Dickel, Eleanor Dunling, Jake Flowerdew, Brian

Kootte, Stephan Malbrunot-Ettenauer, Fernando Maldonado Millán, Ali Mollaebrahami, Erich Leistenschneider, Eleni Marina Lykiardopoulou, Christoph Scheidenberger and A. A. Kwiatkowski.

Funding: This work was funded by the Natural Sciences and Engineering Research Council (NSERC) of Canada and the National Research Council (NRC) of Canada through TRIUMF as well as from the German Federal Ministry for Education and Research (BMBF) under contracts no. 05P19RGFN1 and 05P21RGFN1, the German Research Foundation (DFG) under contract no. 422761894, by HGS-HiRe, by Justus-Liebig-Universität Gießen and GSI under the JLU-GSI strategic Helmholtz partnership agreement.

Acknowledgments: The author wishes to acknowledge and thank M. Good for his expertise in maintaining the TITAN facility and J. Lassen and the TRIUMF laser group for their outstanding work in creating laser schemes and for their tireless hard work.

Conflicts of Interest: The funders had no role in the design of the study; in the collection, analyses, or interpretation of data; in the writing of the manuscript; or in the decision to publish the results.

Abbreviations

The following abbreviations are used in this manuscript:

AME	Atomic Mass Evaluation
EMG	Exponentially Modified Gaussian
IOI	Ion(s) of Interest
ISOL	Isotope Separation On-Line
IT	Isochronous Turn(s)
MLE	Maximum Likelihood Estimator
MR-TOF MS	Multiple-Reflection Time-of-Flight Mass Spectrometer
PPS	Particles Per Second
RFQ	Radio Frequency Quadrupole
RIB	Radioactive Ion Beam
TFS	Time Focus Shift
TITAN	TRIUMF's Ion Trap for Atomic and Nuclear science
TOF	Time-of-Flight
TRC	Time Resolved Calibration
TRILIS	TRIUMF's Resonant Ionization Laser Ion Source

References

1. Reiter, M.; Andrés, S.A.S.; Bergmann, J.; Dickel, T.; Dilling, J.; Jacobs, A.; Kwiatkowski, A.; Plaß, W.; Scheidenberger, C.; Short, D.; et al. Commissioning and performance of TITAN's Multiple-Reflection Time-of-Flight Mass-Spectrometer and isobar separator. *Nuclear Instruments and Methods in Physics Research Section A: Accelerators, Spectrometers, Detectors and Associated Equipment* **2021**, *1018*, 165823. <https://doi.org/https://doi.org/10.1016/j.nima.2021.165823>.
2. Jesch, C.; et al. The MR-TOF-MS isobar separator for the TITAN facility at TRIUMF. *Hyperfine Interact.* **2015**, *235*, 97–106. https://doi.org/10.1007/978-3-319-61588-2_21.
3. Kwiatkowski, A.A.; Dilling, J.; Malbrunot-Ettenauer, S.; Reiter, M.P. 15 years of precision mass measurements at TITAN. *The European Physical Journal A* **2024**, *60*. <https://doi.org/10.1140/epja/s10050-024-01241-6>.
4. Lykiardopoulou, E.; Walls, C.; Bergmann, J.; Brodeur, M.; Brown, C.; Cardona, J.; Czihaly, A.; Dickel, T.; Duguet, T.; Ebran, J.; et al. Refined topology of the $N = 20$ island of inversion with high precision mass measurements of $^{31-33}\text{Na}$ and $^{31-35}\text{Mg}$. *Physical Review Letters* **2024** forthcoming.
5. Paul, S.F.; Bergmann, J.; Cardona, J.D.; Dietrich, K.A.; Dunling, E.; Hockenbery, Z.; Hornung, C.; Izzo, C.; Jacobs, A.; Javaji, A.; et al. Mass measurements of $^{60-63}\text{Ga}$ reduce x-ray burst model uncertainties and extend the evaluated $T = 1$ isobaric multiplet mass equation. *Phys. Rev. C* **2021**, *104*, 065803. <https://doi.org/10.1103/PhysRevC.104.065803>.
6. Dickel, T.; Plaß, W.; Becker, A.; Czok, U.; Geissel, H.; Haettner, E.; Jesch, C.; Kinsel, W.; Petrick, M.; Scheidenberger, C.; et al. A high-performance multiple-reflection time-of-flight mass spectrometer and isobar separator for the research with exotic nuclei. *Nuclear Instruments and Methods in Physics Research Section A: Accelerators, Spectrometers, Detectors and Associated Equipment* **2015**, *777*, 172–188. <https://doi.org/https://doi.org/10.1016/j.nima.2014.12.094>.

7. Yavor, M.I.; Plaß, W.R.; Dickel, T.; Geissel, H.; Scheidenberger, C. Ion-optical design of a high-performance multiple-reflection time-of-flight mass spectrometer and isobar separator. *International Journal of Mass Spectrometry* **2015**, *381–382*, 1–9. <https://doi.org/https://doi.org/10.1016/j.ijms.2015.01.002>.
8. Plaß, W.R.; Dickel, T.; Czok, U.; Geissel, H.; Petrick, M.; Reinheimer, K.; Scheidenberger, C.; I.Yavor, M. Isobar separation by time-of-flight mass spectrometry for low-energy radioactive ion beam facilities. *Nuclear Instruments and Methods in Physics Research Section B: Beam Interactions with Materials and Atoms* **2008**, *266*, 4560–4564. Proceedings of the XVth International Conference on Electromagnetic Isotope Separators and Techniques Related to their Applications, <https://doi.org/https://doi.org/10.1016/j.nimb.2008.05.079>.
9. Schury, P.; Okada, K.; Shchepunov, S.; Sonoda, T.; Takamine, A.; Wada, M.; Wollnik, H.; Yamazaki, Y. Multi-reflection time-of-flight mass spectrograph for short-lived radioactive ions. *Eur. Phys. J. A* **2009**, *42*, 343–349. <https://doi.org/10.1140/epja/i2009-10882-6>.
10. Wolf, R.; Eritt, M.; Marx, G.; Schweikhard, L. A multi-reflection time-of-flight mass separator for isobaric purification of radioactive ion beams. *Hyperfine Interactions* **2011**, *199*, 115–122. <https://doi.org/10.1007/s10751-011-0306-8>.
11. Mardor, I.; Andrés, S.A.S.; Dickel, T.; Amanbayev, D.; Beck, S.; Bergmann, J.; Geissel, H.; Gröf, L.; Haettner, E.; Hornung, C.; et al. Mass measurements of As, Se, and Br nuclei, and their implication on the proton-neutron interaction strength toward the $N = Z$ line. *Phys. Rev. C* **2021**, *103*, 034319. <https://doi.org/10.1103/PhysRevC.103.034319>.
12. Jacobs, A.; Andreoiu, C.; Bergmann, J.; Brunner, T.; Dickel, T.; Dillmann, I.; Dunling, E.; Flowerdew, J.; Graham, L.; Gwinner, G.; et al. Improved high-precision mass measurements of mid-shell neon isotopes. *Nuclear Physics A* **2023**, *1033*, 122636. <https://doi.org/https://doi.org/10.1016/j.nuclphysa.2023.122636>.
13. Leistenschneider, E.; Dunling, E.; Bollen, G.; Brown, B.A.; Dilling, J.; Hamaker, A.; Holt, J.D.; Jacobs, A.; Kwiatkowski, A.A.; Miyagi, T.; et al. Precision Mass Measurements of Neutron-Rich Scandium Isotopes Refine the Evolution of $N = 32$ and $N = 34$ Shell Closures. *Phys. Rev. Lett.* **2021**, *126*, 042501. <https://doi.org/10.1103/PhysRevLett.126.042501>.
14. Beck, S.; Kootte, B.; Dedes, I.; Dickel, T.; Kwiatkowski, A.A.; Lykiardopoulou, E.M.; Plaß, W.R.; Reiter, M.P.; Andreoiu, C.; Bergmann, J.; et al. Mass Measurements of Neutron-Deficient Yb Isotopes and Nuclear Structure at the Extreme Proton-Rich Side of the $N = 82$ Shell. *Phys. Rev. Lett.* **2021**, *127*, 112501. <https://doi.org/10.1103/PhysRevLett.127.112501>.
15. Lykiardopoulou, E.M.; Audi, G.; Dickel, T.; Huang, W.J.; Lunney, D.; Plaß, W.R.; Reiter, M.P.; Dilling, J.; Kwiatkowski, A.A. Exploring the limits of existence of proton-rich nuclei in the $Z = 70 - 82$ region. *Phys. Rev. C* **2023**, *107*, 024311. <https://doi.org/10.1103/PhysRevC.107.024311>.
16. Bricault, P.; Baartman, R.; Dombsky, M.; Hurst, A.; Mark, C.; Stanford, G.; Schmor, P. TRIUMF-ISAC target station and mass separator commissioning. *Nuclear Physics A* **2002**, *701*, 49–53. 5th International Conference on Radioactive Nuclear Beams, [https://doi.org/https://doi.org/10.1016/S0375-9474\(01\)01546-9](https://doi.org/https://doi.org/10.1016/S0375-9474(01)01546-9).
17. Lassen, J.; Bricault, P.; Dombsky, M.; Lavoie, J.P.; Gillner, M.; Gottwald, T.; Hellbusch, F.; Teigelhöfer, A.; Voss, A.; Wendt, K.D.A. Laser Ion Source Operation at the TRIUMF Radioactive Ion Beam Facility. *AIP Conference Proceedings* **2009**, *1104*, 9–15, [https://pubs.aip.org/aip/acp/article-pdf/1104/1/9/11610910/9_1_online.pdf]. <https://doi.org/10.1063/1.3115616>.
18. Brunner, T.; Smith, M.; Brodeur, M.; Ettenauer, S.; Gallant, A.; Simon, V.; Chaudhuri, A.; Lapierre, A.; Mané, E.; Ringle, R.; et al. TITAN's digital RFQ ion beam cooler and buncher, operation and performance. *Nuclear Instruments and Methods in Physics Research Section A: Accelerators, Spectrometers, Detectors and Associated Equipment* **2012**, *676*, 32–43. <https://doi.org/https://doi.org/10.1016/j.nima.2012.02.004>.
19. Plaß, W.R.; Dickel, T.; Andres, S.A.S.; Ebert, J.; Greiner, F.; Hornung, C.; Jesch, C.; Lang, J.; Lippert, W.; Majoros, T.; et al. High-performance multiple-reflection time-of-flight mass spectrometers for research with exotic nuclei and for analytical mass spectrometry. *Physica Scripta* **2015**, *2015*, 014069. <https://doi.org/10.1088/0031-8949/2015/T166/014069>.
20. Ayet San Andrés, S.; Hornung, C.; Ebert, J.; Plaß, W.R.; Dickel, T.; Geissel, H.; Scheidenberger, C.; Bergmann, J.; Greiner, F.; Haettner, E.; et al. High-resolution, accurate multiple-reflection time-of-flight mass spectrometry for short-lived, exotic nuclei of a few events in their ground and low-lying isomeric states. *Phys. Rev. C* **2019**, *99*, 064313. <https://doi.org/10.1103/PhysRevC.99.064313>.

21. Dickel, T.; San Andres, S.; Beck, S.; Bergmann, J.; Dilling, J.; Greiner, F.; Hornung, C.; Jacobs, A.; Kripko-Koncz, G.; Kwiatkowski, A.; et al. Recent upgrades of the multiple-reflection time-of-flight mass spectrometer at TITAN, TRIUMF. *Hyperfine Interactions* **2019**, 240. <https://doi.org/10.1007/s10751-019-1610-y>.
22. Paul, S.F. emgfit - Fitting of time-of-flight mass spectra with hyper-EMG models **2024**. <https://doi.org/10.5281/zenodo.10552901>.
23. Kondev, F.; Wang, M.; Huang, W.; Naimi, S.; Audi, G. The NUBASE2020 evaluation of nuclear physics properties *. *Chinese Physics C* **2021**, 45, 030001. <https://doi.org/10.1088/1674-1137/abddae>.
24. Wang, M.; Huang, W.; Kondev, F.; Audi, G.; Naimi, S. The AME 2020 atomic mass evaluation (II). Tables, graphs and references*. *Chinese Physics C* **2021**, 45, 030003. <https://doi.org/10.1088/1674-1137/abddaf>.
25. Martin, A.; Ackermann, D.; Audi, G.; Blaum, K.; Block, M.; Chaudhuri, A.; Di, Z.; Eliseev, S.; Ferrer, R.; Habs, D.; et al. Mass measurements of neutron-deficient radionuclides near the end-point of the rp-process with SHIPTRAP. *European Physical Journal A* **2007**, 34, 341–348. <https://doi.org/10.1140/epja/i2007-10520-5>.
26. Elomaa, V.V.; Vorobjev, G.K.; Kankainen, A.; Batist, L.; Eliseev, S.; Eronen, T.; Hakala, J.; Jokinen, A.; Moore, I.D.; Novikov, Y.N.; et al. Quenching of the SnSbTe Cycle in the rp Process. *Phys. Rev. Lett.* **2009**, 102, 252501. <https://doi.org/10.1103/PhysRevLett.102.252501>.
27. Schury, P.; Wada, M.; Ito, Y.; Kaji, D.; Arai, F.; MacCormick, M.; Murray, I.; Haba, H.; Jeong, S.; Kimura, S.; et al. First online multireflection time-of-flight mass measurements of isobar chains produced by fusion-evaporation reactions: Toward identification of superheavy elements via mass spectroscopy. *Phys. Rev. C* **2017**, 95, 011305. <https://doi.org/10.1103/PhysRevC.95.011305>.
28. Wienholtz, F.; Beck, D.; Blaum, K.; Borgmann, C.; Breitenfeldt, M.; Cakirli, R.B.; George, S.; Herfurth, F.; Holt, J.D.; Kowalska, M.; et al. Masses of exotic calcium isotopes pin down nuclear forces. *Nature* **2013**, 498, 346–349.
29. Mayer, M.G. On Closed Shells in Nuclei. II. *Phys. Rev.* **1949**, 75, 1969–1970. <https://doi.org/10.1103/PhysRev.75.1969>.
30. Ascher, P.; Daudin, L.; Flayol, M.; Gerbaux, M.; Grévy, S.; Hukkanen, M.; Husson, A.; de Roubin, A.; Alfaut, P.; Blank, B.; et al. PIPERADE: A double Penning trap for mass separation and mass spectrometry at DESIR/SPIRAL2. *Nuclear Instruments and Methods in Physics Research Section A: Accelerators, Spectrometers, Detectors and Associated Equipment* **2021**, 1019, 165857. <https://doi.org/https://doi.org/10.1016/j.nima.2021.165857>.
31. Blaum, K. High-accuracy mass spectrometry with stored ions. *Physics Reports* **2006**, 425, 1–78. <https://doi.org/https://doi.org/10.1016/j.physrep.2005.10.011>.
32. Meisel, Z.; George, S. Time-of-flight mass spectrometry of very exotic systems. *International Journal of Mass Spectrometry* **2013**, 349–350, 145–150. 100 years of Mass Spectrometry, <https://doi.org/https://doi.org/10.1016/j.ijms.2013.03.022>.
33. Mukha, I.; Batist, L.; Becker, F.; Blazhev, A.; Bröchle, A.; Döring, J.; Górski, M.; Grawe, H.; Faestermann, T.; Hoffman, C.; et al. Studies of β -delayed proton decays of $N \simeq Z$ nuclei around 100Sn at the GSI-ISOL facility. *Nuclear Physics A* **2004**, 746, 66–70. Proceedings of the Sixth International Conference on Radioactive Nuclear Beams (RNB6), <https://doi.org/https://doi.org/10.1016/j.nuclphysa.2004.09.065>.
34. Kavatsyuk, O.; Kavatsyuk, M.; Batist, L.; Banu, A.; Becker, F.; Blazhev, A.; Bröchle, W.; Döring, J.; Faestermann, T.; Górski, M.; et al. Beta decay of ^{103}Sn . *The European Physical Journal A - Hadrons and Nuclei* **2005**, 25, 211–222.
35. Huang, W.; Wang, M.; Kondev, F.; Audi, G.; Naimi, S. The AME 2020 atomic mass evaluation (I). Evaluation of input data, and adjustment procedures*. *Chinese Physics C* **2021**, 45, 030002. <https://doi.org/10.1088/1674-1137/abddb0>.
36. Hardy, J.; Carraz, L.; Jonson, B.; Hansen, P. The essential decay of pandemonium: A demonstration of errors in complex beta-decay schemes. *Physics Letters B* **1977**, 71, 307–310. [https://doi.org/https://doi.org/10.1016/0370-2693\(77\)90223-4](https://doi.org/https://doi.org/10.1016/0370-2693(77)90223-4).
37. Hoff, P.; Aleklett, K.; Lund, E.; Rudstam, G. Decay schemes and total decay energies of ^{89}Br and ^{90}Br . *Zeitschrift für Physik A Atoms and Nuclei* **1981**, 300, 289–298.
38. Rahaman, S.; Hager, U.; Elomaa, V.V.; Eronen, T.; Hakala, J.; Jokinen, A.; Kankainen, A.; Karvonen, P.; Moore, I.D.; Penttilä, H.; et al. Precise atomic masses of neutron-rich Br and Rb nuclei close to the r-process path. *The European Physical Journal A* **2007**, 32, 87–96.

39. Delahaye, P.; Audi, G.; Blaum, K.; Carrel, F.; George, S.; Herfurth, F.; Herlert, A.; Kellerbauer, A.; Kluge, H.J.; Lunney, D.; et al. High-accuracy mass measurements of neutron-rich Kr isotopes. *Phys. Rev. C* **2006**, *74*, 034331. <https://doi.org/10.1103/PhysRevC.74.034331>.
40. Porter, W.S.; Ashrafxhani, B.; Bergmann, J.; Brown, C.; Brunner, T.; Cardona, J.D.; Curien, D.; Dedes, I.; Dickel, T.; Dudek, J.; et al. Mapping the $N = 40$ island of inversion: Precision mass measurements of neutron-rich Fe isotopes. *Phys. Rev. C* **2022**, *105*, L041301. <https://doi.org/10.1103/PhysRevC.105.L041301>.
41. Dilling, J.; Blaum, K.; Brodeur, M.; Eliseev, S. Penning-Trap Mass Measurements in Atomic and Nuclear Physics. *Annual Review of Nuclear and Particle Science* **2018**, *68*, 45–74. <https://doi.org/10.1146/annurev-nucl-102711-094939>.
42. Gallant, A.T.; Bale, J.C.; Brunner, T.; Chowdhury, U.; Ettenauer, S.; Lennarz, A.; Robertson, D.; Simon, V.V.; Chaudhuri, A.; Holt, J.D.; et al. New Precision Mass Measurements of Neutron-Rich Calcium and Potassium Isotopes and Three-Nucleon Forces. *Phys. Rev. Lett.* **2012**, *109*, 032506. <https://doi.org/10.1103/PhysRevLett.109.032506>.
43. Borello-Lewin, T.; Dietzsch, O. Binding Energies in Zr from (d, p) and (d, t) Reactions. *Z. Naturforsch* **1979**, pp. 1536–1537.
44. Johnson, C.H.; Trail, C.C.; Galonsky, A. Thresholds for (p, n) Reactions on 26 Intermediate-Weight Nuclei. *Phys. Rev.* **1964**, *136*, B1719–B1729. <https://doi.org/10.1103/PhysRev.136.B1719>.
45. Okano, K.; Nishimura, K. (p, n) Threshold Measurements on Na, Al, Cu, Ga, Ge, Se, Y, and Sn. *Journal of the Physical Society of Japan* **1963**, *18*, 1563–1568, [<https://doi.org/10.1143/JPSJ.18.1563>]. <https://doi.org/10.1143/JPSJ.18.1563>.
46. Hamilton, J.H.; Langer, L.M.; Smith, W.G. Evidence for Small Deviations in the Allowed Positron Spectrum of Zr^{89} . *Phys. Rev.* **1960**, *119*, 772–776. <https://doi.org/10.1103/PhysRev.119.772>.
47. Reiter, M.; Ames, F.; Andreoiu, C.; Ayet San Andrés, S.; Babcock, C.; Barquest, B.; Bergmann, J.; Bollig, J.; Brunner, T.; Dickel, T.; et al. Improved beam diagnostics and optimization at ISAC via TITAN's MR-TOF-MS. *Nuclear Instruments and Methods in Physics Research Section B: Beam Interactions with Materials and Atoms* **2020**, *463*, 431–436. <https://doi.org/https://doi.org/10.1016/j.nimb.2019.04.034>.

Disclaimer/Publisher's Note: The statements, opinions and data contained in all publications are solely those of the individual author(s) and contributor(s) and not of MDPI and/or the editor(s). MDPI and/or the editor(s) disclaim responsibility for any injury to people or property resulting from any ideas, methods, instructions or products referred to in the content.